

Metastasis Stimulation by Hypoxia and Acidosis-Induced Extracellular Lipid Uptake Is Mediated by Proteoglycan-Dependent Endocytosis

Julien A. Menard¹, Helena C. Christianson¹, Paulina Kucharzewska¹, Erika Bourseau-Guilmain¹, Katrin J. Svensson², Eva Lindqvist¹, Vineesh Indira Chandran¹, Lena Kjellén³, Charlotte Welinder^{1,4}, Johan Bengzon^{5,6}, Maria C. Johansson¹, and Mattias Belting^{1,7}

Abstract

Hypoxia and acidosis are inherent stress factors of the tumor microenvironment and have been linked to increased tumor aggressiveness and treatment resistance. Molecules involved in the adaptive mechanisms that drive stress-induced disease progression constitute interesting candidates of therapeutic intervention. Here, we provide evidence of a novel role of heparan sulfate proteoglycans (HSPG) in the adaptive response of tumor cells to hypoxia and acidosis through increased internalization of lipoproteins, resulting in a lipid-storing phenotype and enhanced tumor-forming capacity. Patient glioblastoma tumors and cells under hypoxic and acidic stress acquired a lipid droplet (LD)-loaded phenotype, and showed an increased recruitment of all major lipoproteins, HDL, LDL, and VLDL. Stress-induced LD accumulation was associated with increased spheroid-forming capacity during reoxygenation

in vitro and lung metastatic potential *in vivo*. On a mechanistic level, we found no apparent effect of hypoxia on HSPGs, whereas lipoprotein receptors (VLDLR and SR-B1) were transiently up-regulated by hypoxia. Importantly, however, using pharmacologic and genetic approaches, we show that stress-mediated lipoprotein uptake is highly dependent on intact HSPG expression. The functional relevance of HSPG in the context of tumor cell stress was evidenced by HSPG-dependent lipoprotein cell signaling activation through the ERK/MAPK pathway and by reversal of the LD-loaded phenotype by targeting of HSPGs. We conclude that HSPGs may have an important role in the adaptive response to major stress factors of the tumor microenvironment, with functional consequences on tumor cell signaling and metastatic potential. *Cancer Res*; 76(16); 4828–40. ©2016 AACR.

Introduction

Solid malignant tumors are characterized by severe hypoxic and acidic stress as a consequence of uncontrolled proliferation and survival, resulting in a structurally and functionally abnormal microenvironment. Stress factors are major drivers of cancer progression providing a strong selective pressure asso-

ciated with decreased patient survival and intrinsic resistance to conventional oncologic treatments (1–3). A more detailed understanding of how adaptive responses to the microenvironment drive tumor progression is critical for the development of more rational therapeutic strategies of cancer (4, 5).

Adaptive responses to stress may include angiogenesis, immune cell evasion, coagulation activation, and dedifferentiation into stemness phenotypes, but also abnormal cell metabolism. Tumor cells undergo a significant shift from oxidative phosphorylation in mitochondria toward anaerobic glycolysis, including the induction of glucose transporters (GLUT), glycolytic enzymes and lactate dehydrogenase, as well as increased synthesis of glycogen, lipids, and phosphorylated lipid metabolites (6). Oncogene-driven induction of glucose uptake through GLUTs and increased glycolytic flux at normoxic conditions is known as the Warburg effect (7), a phenomenon that in many ways is potently reinforced by hypoxia (8, 9). This further leads to the acidification of the extracellular microenvironment through the action of, for example, carbonic anhydrases, sodium-proton exchange, and monocarboxylate transport proteins that significantly contribute to the invasive and metastatic potential of tumor cells (5, 10). Accumulating evidence supports an important role of increased functional activity of cell surface transport and receptor proteins in tumor development (11), and hypoxia-driven malignant progression

¹Department of Clinical Sciences, Section of Oncology and Pathology, Lund University, Lund, Sweden. ²Dana-Farber Cancer Institute and Department of Cell Biology, Harvard Medical School, Boston, Massachusetts. ³Department of Medical Biochemistry and Microbiology, Science for Life Laboratory, Uppsala University, Uppsala, Sweden. ⁴Center of Excellence in Biological and Medical Mass Spectrometry "CEBMMS", Biomedical Centre D13, Lund University, Lund, Sweden. ⁵Lund Stem Cell Center, Lund University, Lund, Sweden. ⁶Department of Clinical Sciences, Section of Neurosurgery, Lund University, Lund, Sweden. ⁷Skåne University Hospital, Lund, Sweden.

Note: Supplementary data for this article are available at Cancer Research Online (<http://cancerres.aacrjournals.org/>).

Corresponding Author: Mattias Belting, Department of Clinical Sciences, Section of Oncology and Pathology, Lund University, Barngatan 2B, Lund SE-221 85, Sweden. Phone: 464-617-8549; Fax: 464-617-6023; E-mail: Mattias.Belting@med.lu.se

doi: 10.1158/0008-5472.CAN-15-2831

©2016 American Association for Cancer Research.

has been shown to be directly related to deregulated endocytosis and receptor protein trafficking (12). How hypoxia and acidosis may increase tumor aggressiveness through abnormal endocytosis of extracellular nutrient sources such as lipoproteins remains to be explored.

Here, we were interested in investigating how the endocytic lipid transport machinery at the mechanistic and functional level may be involved in cancer cell adaptation to hypoxic and acidic stress to better understand how to target aggressive tumors.

Materials and Methods

Descriptions of fluorescence and electron microscopy, laser capture microdissection, gene microarray, and qRT-PCR, HS composition, LDL aggregation, lipid quantitation, label-free lipoprotein receptor quantification by LC/MS-MS, Western blotting, and phospho-kinase array are provided in Supplementary Information. The gene microarray data reported in this article have been deposited in the Gene Expression Omnibus (GEO) database, www.ncbi.nlm.nih.gov/geo (accession no. GSE45301).

Cells and clinical samples

Human glioblastoma (U87-MG; HTB-14, ATCC), cervical cancer (HeLa; CCL-2, ATCC), mouse Lewis lung carcinoma (LLC1; CRL-1642, ATCC), glioma [GL261, from the original laboratory (13) and kindly provided by Dr. Anna Darabi, Lund University, Lund, Sweden], wild-type Chinese hamster ovary (CHO-K1; CCL-61, ATCC), PG-deficient (pgsA-754; CRL-2242, ATCC), N-sulfation-deficient, and 2-O-sulfation-deficient (pgsE-606 and pgsF-17; kindly provided by Dr. J.D. Esko, University of California San Diego, San Diego, CA), and mouse embryonic fibroblasts (MEF; CF-1, ATCC) were used. Cell lines were freshly purchased from ATCC (during 2012–2016), authenticated by STR DNA profiling (ATCC), and passaged <6 months after receipt or resuscitation. GL261 cells were authenticated by us (during 2013–2016) by their typical glioblastoma tumor morphology when injected into the brains of syngeneic C57/BL6 mice, and pgsE and pgsF-17 cells (during 2012–2016) by their deficient staining with anti-HS antibodies. All cell lines were regularly checked negative for mycoplasma using the EZ-PCR mycoplasma kit (Biological Industries). Cells were routinely cultured in F12-K (Gibco, Life Technologies; CHO cells) or high-glucose DMEM (HyClone, GE) medium supplemented with 10% (v/v) FBS (Sigma Aldrich-F7524), 2 mmol/L L-glutamine (Sigma Aldrich, G7513), 100 U/mL penicillin, and 100 µg/mL streptomycin (PEST; Sigma Aldrich, P0781), referred to as "full medium," in 21% O₂, 5% CO₂, humidified incubators. For hypoxia experiments, cells were incubated in a SCI-TIVE N-N hypoxia workstation (Baker Ruskinn) set at 1% O₂ and 5% CO₂. Tumor specimens were from patients with primary astrocytoma grade II and glioblastoma grade IV (according to WHO) at the Department of Neurosurgery, Lund University (Lund, Sweden). Biopsies were collected with informed consent according to Protocol H15642/2008 approved by the Lund University Regional Ethics Board.

Flow cytometry

Lipoprotein uptake and cell surface binding. Human native, 1,1'-dioctadecyl-3,3,3'-tetramethylindocarbocyanine perchlorate (DiI)-labeled HDL, LDL and VLDL were from Intracel Inc., USA. For uptake studies, 5×10^4 cells were seeded in 48-well plates overnight in full medium, followed by switching to

serum-free medium, and incubation at normoxia or hypoxia. In acidosis experiments, the serum-free medium was adjusted to the different pH values using concentrated NaOH and HCl. DiI-lipoproteins in fresh serum-free medium were then added to the cells and uptake was performed for 30 minutes with continued treatments, as specified. Cells were washed extensively with ice-cold PBS, detached with 0.25% trypsin-EDTA (Sigma Aldrich), followed by trypsin neutralization with full medium and PBS wash $\times 2$ prior to FACS analysis in PBS/0.5% BSA, 5 mmol/L EDTA, on an Accuri-C6 flow cytometer (BD Biosciences). The data were acquired with the C6Flow Sampler software (BD Biosciences) and statistical analysis was performed with GraphPad Prism6 software. Cells were kept at 4°C throughout the preparation. In some cases, heparin (Sigma Aldrich, H3393) was added to the lipoprotein solution just prior to addition to cells. For HSPG sulfation inhibition experiments, cells were pretreated with sodium chlorate (25 mmol/L, Alfa Aesar, 044408) or sodium chloride control medium (25 mmol/L Sigma Aldrich, S7653) for 24 hours prior to and during incubation with DiI-lipoprotein.

For lipoprotein cell surface binding, adherent cells were grown in normoxia or hypoxia and detached as described above, counted and transferred to FACS tubes at 2×10^5 cells/300 µL serum-free medium supplemented with DiI-lipoproteins (20 µg/mL final concentration), and incubated on ice for 30 minutes under agitation. Cells were then extensively washed in ice-cold PBS and processed for flow cytometry analysis as described above.

For anti-HS antibody, cell surface binding, cells were grown in normoxia or hypoxia, detached, and incubated with AO4B08 anti-HS antibody (kindly provided by Dr. T.H. van Kuppevelt, University of Nijmegen, Nijmegen, the Netherlands; titer 1:20; ref. 14), then washed in PBS 0.5% BSA and incubated with mouse anti-vsv antibody (Sigma Aldrich-P5D4; 1:500) that recognizes the vsv-epitope of AO4B08, followed by washing in PBS 0.5% BSA and incubation with goat anti-mouse-AF488 antibody (Life Technologies; 1:200). All antibody incubations were performed for 30 minutes on ice. For anti-HS antibody uptake experiments, AO4B08 (1:20), mouse anti-vsv (1:500), and goat anti-mouse-AF488 antibodies (1:200) were precomplexed in serum-free medium at 20°C for 30 minutes, and then incubated with normoxic or hypoxic cells at 37°C for 1 hour. Controls without AO4B08 primary antibody were included in all binding and uptake experiments. Cells were processed for flow cytometry analyses as described above.

Spheroid formation

U87-MG cells were grown in hypoxia for 72 hours in the presence or absence of LDL (50 µg/mL), detached by mild trypsinization and resuspended at a concentration of 1.5×10^4 cells/30 µL in serum-free medium. Thirty microliter drops were used to initiate cell aggregation by the hanging drop method in 35×10 cm dishes (Nunc, Thermo Scientific). After 48 hours of incubation in maintained hypoxia or returned to normoxia (reoxygenation), images of representative drops ($n = 8$ per condition) were acquired using a Zeiss PrimoVert microscope (4× objective) and analyzed by ImageJ.

Lung metastasis

Experimental procedures were approved by the ethical committee for animal research in Malmö/Lund, Sweden (ethical

permit M144-14) and were performed in accordance with the European Union animal rights and ethics directives. Seven- to 9-week-old female NOD-SCID mice received tail vein injections with 1×10^6 LLC1 cells pretreated in the absence or presence of LDL (50 $\mu\text{g/mL}$) for 48 hours at hypoxia. After 14 days, mice were sacrificed and lungs were immediately taken, washed twice in PBS, weighed and fixed in Bouin solution (Sigma Aldrich, HT10132) for 24 hours. Lung surface metastatic foci were counted using an Mz125 dissecting microscope and DFC280 camera (Leica), followed by dissection of separate lobes, paraffin embedding, and hematoxylin/eosin (H&E) staining according to standard protocols. Representative pictures of H&E-stained lung sections (equatorial) were acquired using a BX53 microscope (4 \times and 10 \times objectives) and UC30 camera (Olympus).

Statistical analysis

Statistical significance was tested using the Student *t* test for mean comparison between groups. A $P < 0.05$ was considered statistically significant. Error bars show SD.

Results

Lipid loading at stress conditions is associated with a protumorigenic phenotype

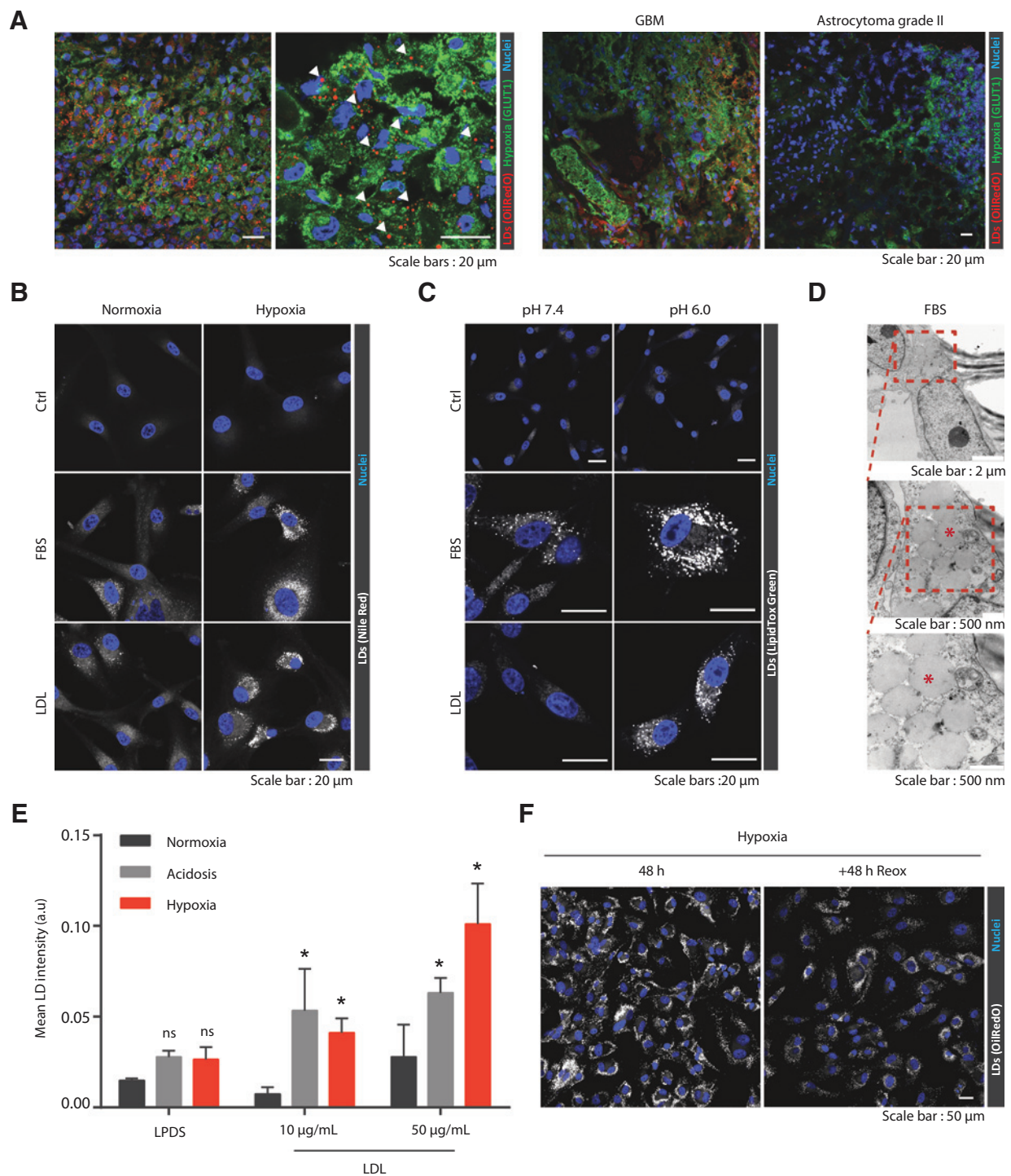
Malignant tumors including glioblastoma, that is, highly aggressive primary brain tumors characterized by profound hypoxia and acidosis, can accumulate lipid droplets (LD; ref. 15). We found that LD accumulation was closely associated with hypoxic areas of patient glioblastoma tumors, as determined by staining for the hypoxia marker GLUT1 (Fig. 1A, left). Low-grade astrocytomas that are devoid of hypoxia-associated necrosis and endothelial hyperproliferation displayed relatively few LDs (Fig. 1A, right). We chose the well-characterized U87-MG cell line established from a glioblastoma patient (16) for further *in vitro* experiments. Glioblastoma cells showed hypoxic induction of the LD-loaded phenotype through mechanisms apparently dependent on extracellular lipids, either from serum or lipoproteins (Fig. 1B). Hypoxic induction of LDs was supported by gene array studies, showing hypoxic upregulation of several gene transcripts associated with LD formation (Supplementary Fig. S1A), most notably hypoxia-inducible protein-2 and adipocyte differentiation-related protein (17). Acidosis is another common stress phenomenon of aggressive tumors that may acquire an extracellular pH down to <6.0 (5, 10). Incubation at acidosis profoundly induced LDs, an effect that also appeared dependent on extracellular lipid (Fig. 1C). We found comparable LD phenotypes in additional cancer cell types, including HeLa, GL261, and LLC1 cells (Supplementary Fig. S1B). Electron microscopy confirmed that structures positive for lipophilic dyes in confocal fluorescence microscopy (Fig. 1B and C) represented LDs displaying a phospholipid monolayer (Fig. 1D). We next treated normoxic, hypoxic, and acidic cells with lipoprotein-deficient serum (LPDS) or different concentrations of LDL, followed by quantitative LD imaging analysis (Fig. 1E). LPDS had no significant effect on LDs, whereas LDL significantly increased LDs both at acidosis and hypoxia, in the latter case in a dose-dependent manner. At the conditions used, cell medium pH remained stable at hypoxia (Supplementary Fig. S1C), and we found no evidence of LDL aggregation (Supplementary Fig. S1D and S1E). The hypoxic

LD phenotype was not reflecting an irreversible preapoptotic stage, as cells remained viable (Supplementary Fig. S1F) and showed efficient LD consumption after reoxygenation (Fig. 1F). Moreover, hypoxia has been shown to induce triglyceride (TG)-rich LDs through mechanisms that involve increased uptake of fatty acids, increased TG synthesis, and decreased β -oxidation (18). However, we found no evidence of increased TGs by LDL treatment in hypoxic cells (Supplementary Fig. S2A), whereas cholesteryl esters were increased both in cells and in isolated LDs (Supplementary Fig. S2B and S2C), indicating that LD accumulation was dependent on extracellular LDL particle-derived cholesterol uptake.

We explored the potential functional relevance of hypoxia-induced LD accumulation using the spheroid formation assay, which has been shown to provide relevant *in vitro* information with respect to tumor metastasis (19–21). When cells were maintained in hypoxia, cell aggregation by LD-loaded as compared with LD-deficient cells appeared increased, although not reaching statistical significance ($P = 0.15$; Fig. 2A). Oxygen levels in tumors are known to fluctuate due to vascular remodeling, and metastatic cells that enter the circulation are exposed to a relatively well oxygenated environment. We found that cell aggregation at reoxygenation was significantly increased when cells were allowed to form LDs in the preceding hypoxic phase (Fig. 2A). To investigate whether this finding could be translated to *in vivo* conditions, we next employed a hematogenous lung metastasis model. Interestingly, the metastatic capacity of hypoxic cells with LDs at the time of intravenous administration was substantially increased as compared with LD-deficient cells, as shown by final lung weight (Fig. 2B) and number of lung surface metastatic foci (Fig. 2C and D). We conclude that stress conditions in the context of extracellular lipoprotein availability induce LD accumulation that is reversible upon reoxygenation, resulting in an increased tumorigenic potency, as evidenced by enhanced spheroid formation and hematogenous metastasis.

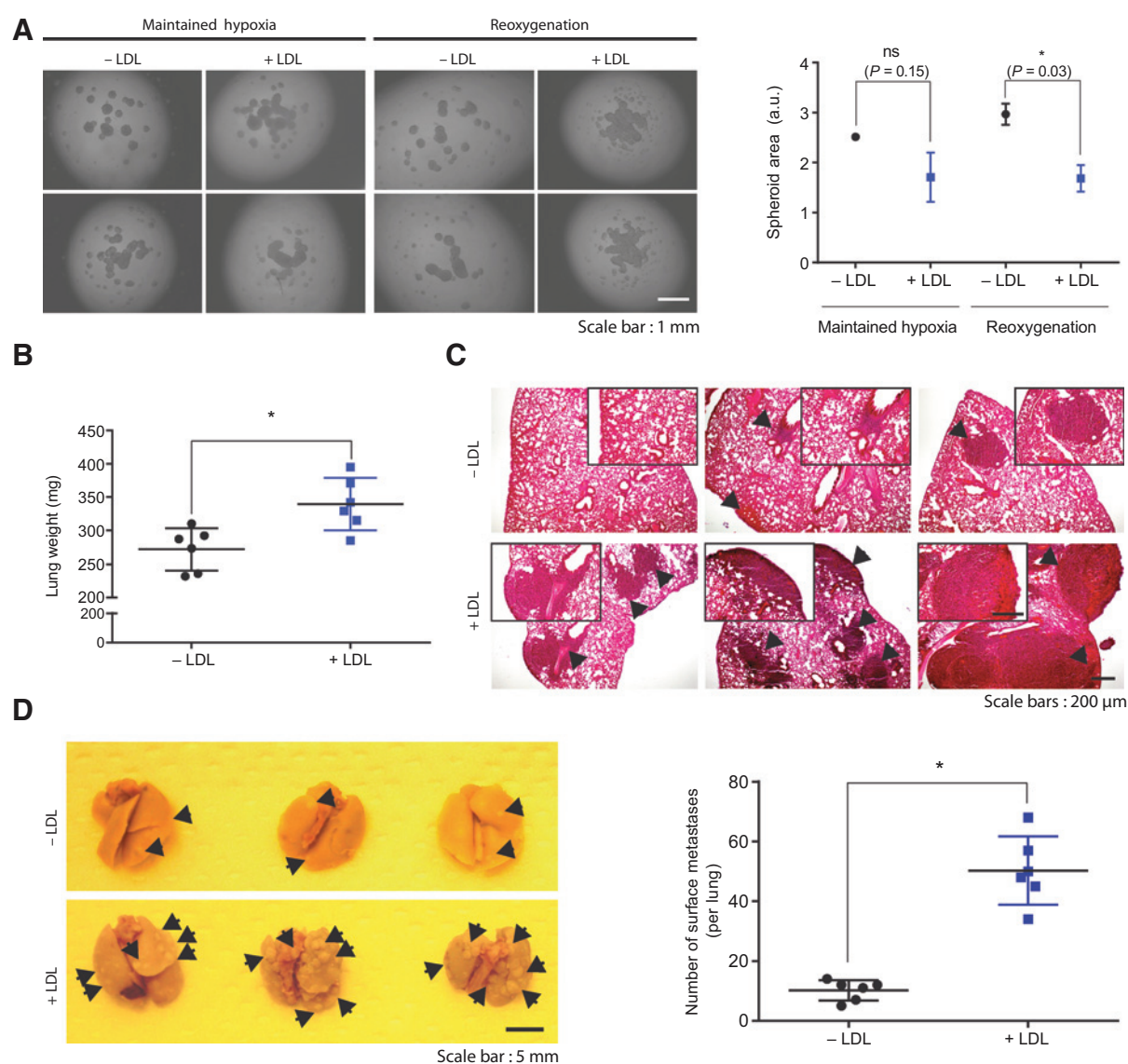
Lipoprotein uptake is induced by hypoxic and acidic stress

We set out to determine how hypoxia and acidosis regulate lipoprotein transport in glioblastoma cells, using human native lipoproteins fluorescently labeled with 1,1'-dioctadecyl-3,3,3',3'-tetramethylindocarbocyanine perchlorate (DiI). Confocal microscopy suggested that the endocytosis of VLDL as well as LDL was increased by hypoxia (Fig. 3A). Extensive, quantitative studies by flow cytometry showed that hypoxia induced the uptake of all major classes of lipoproteins, VLDL, LDL, and HDL over a wide range of concentrations (Fig. 3B). Hypoxic induction of lipoprotein uptake was not restricted to U87-MG cells (Supplementary Fig. S3A and S3B). The specificity of lipoprotein uptake was confirmed by efficient inhibition by incubation at 4°C (Supplementary Fig. S3C) and by an excess of unlabeled lipoprotein (Supplementary Fig. S3D). In addition to receptor-mediated uptake, lipoproteins may be internalized through macropinocytosis, resulting in LD accumulation in macrophages (22). However, we found no increase but rather a slight decrease of macropinocytic activity by hypoxia, as assessed by dextran uptake (Supplementary Fig. S3E and S3F). Notably, the hypoxic effect on VLDL and LDL uptake was transient, and was comparable with normoxic conditions at 24 hours (Fig. 3C). We could also show that acidic stress is associated with increased uptake of LDL as well as VLDL in glioblastoma and MEF cells (Fig. 3D and E). The effect was shown to be indirect when

**Figure 1.**

Stress-induced LD loading depends on exogenous lipids. **A**, glioblastoma patient tumors stained for hypoxia (GLUT1, green) and LDs (white arrowheads; red). Astrocytoma grade II displayed less hypoxia and LD accumulation. Blue, DAPI nuclear stain. **B** and **C**, U87-MG cells were incubated in normoxia or hypoxia (**B**) or at neutral or acidic pH (**C**) in serum-free medium (Ctrl) supplemented with LDL (50 μ g/mL) or FBS (10%) and analyzed by confocal microscopy. Hoechst nuclear stain (blue); Nile red or LipidTox LD stain, as indicated (white). Shown are representative images of at least three independent experiments. **D**, transmission electron microscopy of a representative field of U87-MG cells grown for 48 hours in hypoxia in the presence of extracellular lipids (10% FBS). **E**, U87-MG cells were grown in normoxia, hypoxia, or acidosis (pH 6.0) in medium supplemented with LPDS or in the presence of LDL (10 and 50 μ g/mL). Quantification of LD loading using CellProfiler was performed as described in Supplementary Information. Data are presented as the mean \pm SD from triplicate experiments, $n \geq 51$ cells per condition. *, $P < 0.05$. ns, nonsignificant. **F**, staining for LDs (white) in U87-MG cells incubated in hypoxia in the presence of LDL (50 μ g/mL), and following reoxygenation (Reox). Shown are representative fields of at least three independent experiments.

Menard et al.

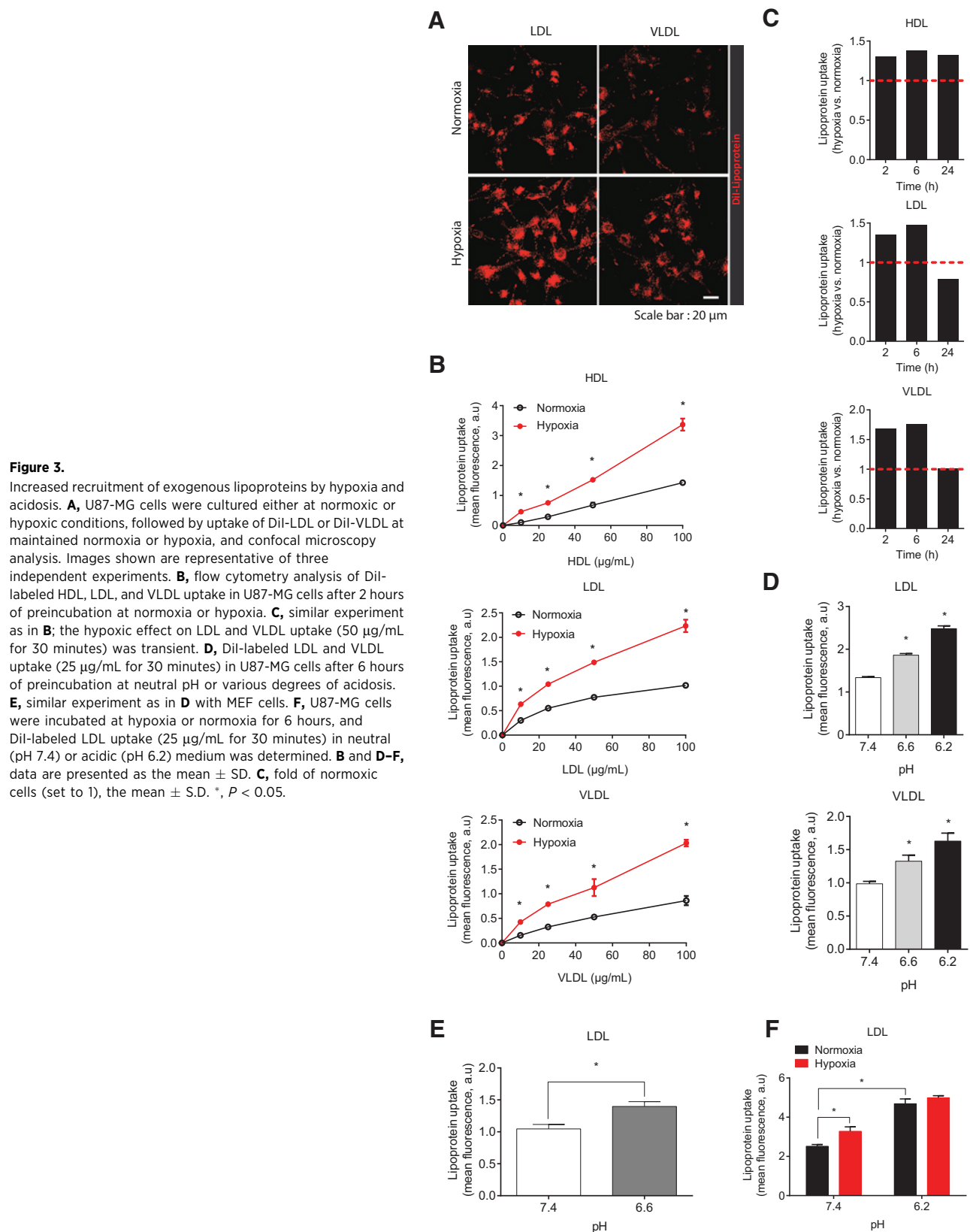
**Figure 2.**

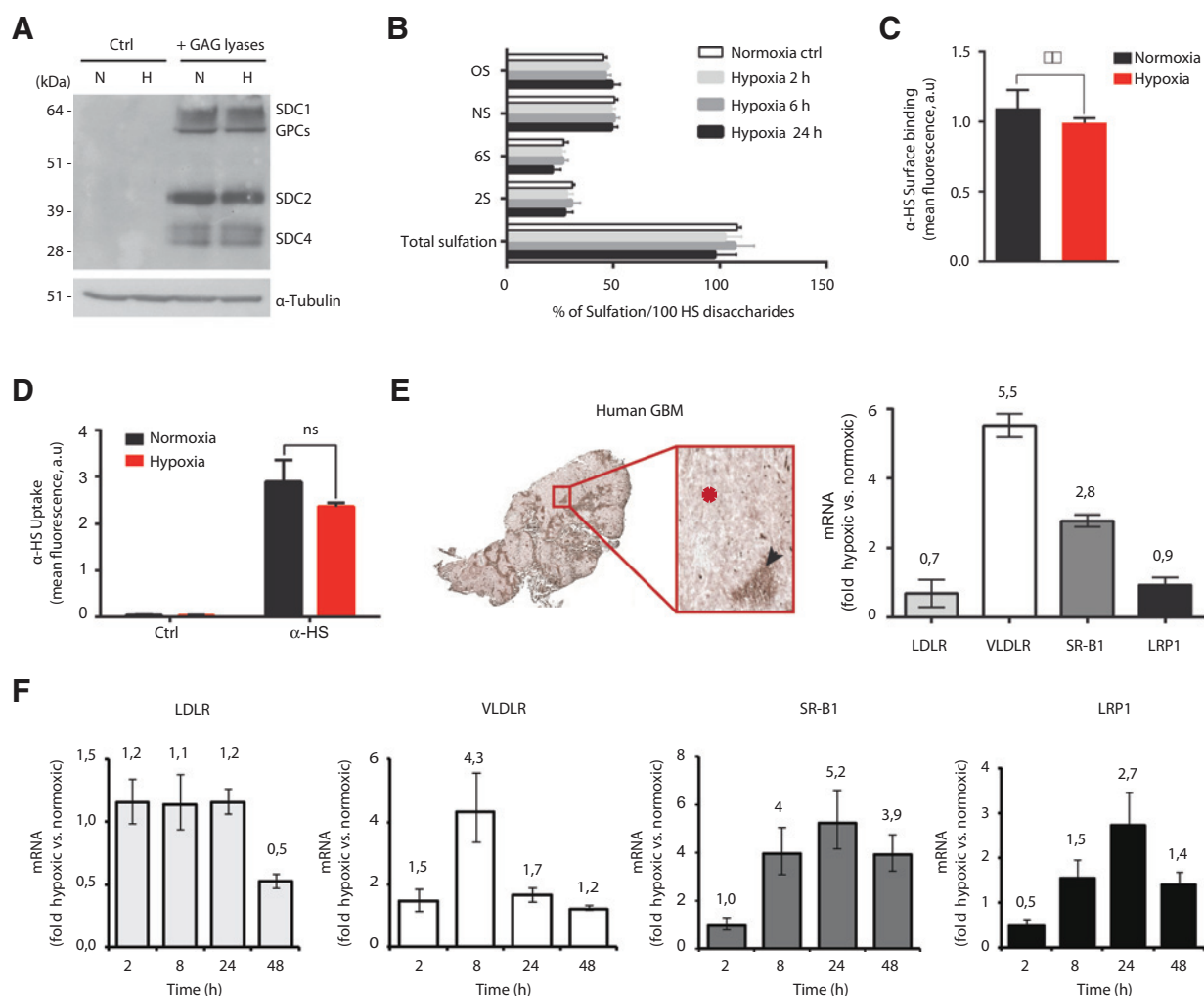
Enhanced spheroid formation and metastatic potential of hypoxic cells with the LD-loaded phenotype. **A**, U87-MG cells were grown at hypoxia in the absence or presence of LDL (50 μ g/mL), followed by the spheroid formation assay either in maintained hypoxia or at normoxic conditions (Reoxygenation). Left, shown are two representative images per condition from three independent experiments. Right, quantification of spheroid area, which is inversely related to spheroid-forming capacity using ImageJ. Data are presented as the mean \pm SD from two independent experiments, each performed in quadruplicates. *, $P < 0.05$. **B**, LLC1 cells were grown at hypoxia either in the absence or presence of LDL (50 μ g/mL), and injected intravenously in SCID mice. Final lung weight from mice of the respective groups ($n = 6$) was determined. **C**, shown are three representative sections from isolated lungs from the experiment described in **B**. **D**, left, shown are three representative lungs per group from experiment described in **B**. Arrows, lung surface metastases. Right, quantification of metastatic foci. Data are presented as the mean no. of metastases/lung \pm SD ($n = 12$).

cells were preincubated at acidic conditions (Fig. 3D and E) as well as direct when lipoprotein uptake was performed in low-pH medium (Fig. 3F). Moreover, we found no additional effect of hypoxia on acidosis-stimulated lipoprotein uptake (Fig. 3F).

Lipoproteins are internalized by endocytosis via binding to lipoprotein receptors (VLDLR, LDLR, LRP1) and scavenger receptors (SR-B1). The heparan sulfate proteoglycan (HSPG) pathway is involved in the endocytosis of numerous macromolecular ligands (23), and a complex cross-talk between lipoprotein receptors and cell surface HSPGs has been established in non-

malignant cells (23–25). To gain increased mechanistic understanding of how stress induces lipoprotein uptake, we investigated the effects of hypoxia on the overall expression of major cell surface HSPG proteins (syndecans and glypicans). We employed the pan-HSPG antibody 3G10 that specifically recognizes HSPG core proteins (Supplementary Fig. S4A); however, at conditions associated with increased lipoprotein uptake, we found no apparent effect of hypoxia (Fig. 4A). We next performed structural analyses of HS polysaccharides of normoxic and hypoxic glioblastoma cells, and found no significant effect of



**Figure 4.**

Effects of hypoxia on HSPG and lipoprotein receptor expression. **A**, U87-MG cells were incubated in normoxia or hypoxia for 6 hours and were then either untreated (Ctrl) or treated with heparanase III and ABC lyases (+GAG lyases). HSPG core proteins were visualized by immunoblotting with 3G10-antibody. Nondigested controls confirmed the specificity of the 3G10 antibody. **B**, U87-MG cells were grown in normoxia or hypoxia for the indicated time periods, and HS chains were processed for disaccharide composition analysis. **C** and **D**, cells were incubated at normoxia or hypoxia for 2 hours and then either surface-stained at 4°C with AO4B08 anti-HS antibody (α-HS; **C**) or incubated at 37°C for 30 minutes to allow for α-HS internalization (**D**). Controls (Ctrl) are with fluorophore-labeled secondary antibody alone. Flow cytometry data are presented as the mean ± SD. ns, nonsignificant. **E**, laser capture microdissected hypoxic (arrow) and normoxic (red star) regions of glioblastoma patient tumors were analyzed by qRT-PCR. **F**, U87-MG cells were incubated at normoxia or hypoxia for the indicated time periods and analyzed for the level of lipoprotein receptor mRNAs by qRT-PCR. Data are presented as fold increase in hypoxia as compared with normoxia ± SD and are representative of three independent experiments. Values above bars indicate fold change in hypoxia.

hypoxia (Fig. 4B). These results were corroborated by binding and internalization experiments with the anti-HS antibody AO4B08, which recognizes the internalizing HSPG population (26). Neither binding (Fig. 4C) nor uptake (Fig. 4D) of AO4B08 were affected at conditions of hypoxia-induced lipoprotein uptake. In accordance with the lack of a hypoxic effect on HSPG expression, lipoprotein cell surface binding was not affected by hypoxia (Supplementary Fig. S4B and S4C). Laser capture microdissection of hypoxic and normoxic regions of glioblastoma patient tumors (Fig. 4E) as well as *in vitro* gene array data (Supplementary Fig. S5A) and real-time PCR experiments with glioblastoma cells (Fig. 4F) could, however, show hypoxic induction of VLDLR, SR-B1, and LRP1 mRNAs, whereas LDLR was not

induced. To validate mRNA expression data, we next performed label-free quantitative LC/MS-MS where LRP-1, VLDLR, and SR-B1 peptides were subjected to MS1 filtering using the publicly available software Skyline (<http://proteome.gs.washington.edu/software/skyline>; ref. 27). VLDLR and SR-B1 were not detected, probably due to low abundance, whereas LRP1 peptides all were unaffected by hypoxia at conditions of increased lipoprotein uptake (6 hours of hypoxia; Supplementary Table S1). LC-MS/MS data was further supported by Western blot analysis, showing no LRP1 induction (Supplementary Fig. S5B). More importantly, immunoblotting experiments suggested hypoxic induction of VLDLR (Supplementary Fig. S5C) and SR-B1 (Supplementary Fig. S5D) proteins. Together, these results provide

evidence that stress-induced LD loading is associated with the induction of lipoprotein uptake in tumor cells, and suggest that this effect correlates with an increased expression of VLDLR and SR-B1, whereas the level and structure of HSPGs are not directly affected. As there was no evidence of lipoprotein aggregation in the cell medium (Supplementary Fig. S1D and S1E), we conclude that SR-B1 and VLDLR are implied to be important in hypoxia-induced uptake of VLDL, whereas SR-B1 should be involved in the increased uptake of LDL and HDL.

Role of HSPGs in stress-induced lipoprotein uptake

We were interested in exploring the potential functional role of HSPGs in tumor cell stress adaptation, as previous studies with nonmalignant cells have recognized HSPGs as high capacity, global lipoprotein-binding molecules that can act upstream of lipoprotein receptors (23–25). First, we could show that the hypoxic effect on LDL uptake in glioblastoma cells was efficiently reversed by heparin, that is, an HS mimetic (Fig. 5A). Next, lipoprotein uptake experiments were performed with wild-type (CHO-K1) and mutant, PG-deficient (pgsA-745) CHO cells deficient in xylosyl transferase that catalyzes the first step in PG assembly. PgsA cells express approximately 5% PG as compared with wild-type cells (28). We found that also CHO cells respond to hypoxia by increased uptake of LDL (Fig. 5B) as well as VLDL (Supplementary Fig. S5E). More importantly, the hypoxic effect on both LDL and VLDL uptake was efficiently reversed by treatment with heparin (Fig. 5B and Supplementary Fig. S5E). Interestingly, hypoxia-dependent uptake of both lipoprotein types was attenuated in PG-deficient cells (Fig. 5C and D), which was further supported by confocal microscopy (Fig. 5E). PgsA cells are pan-PG deficient, that is, they lack PGs of the HS as well as the chondroitin sulfate type. To specifically investigate the role of HSPGs, we next performed experiments with CHO cell mutants with defective HS *N*-sulfation (pgsE) and 2-*O*-sulfation (pgsF), respectively (29, 30). Also in these mutants, hypoxia failed to significantly affect the uptake of LDL (Fig. 5F, top) as well as VLDL (Fig. 5F, bottom). These results indicate that the hypoxic effect of LDL/VLDL uptake depends on HSPG-assisted uptake. Similarly, acidosis-mediated induction of lipoprotein uptake in glioblastoma cells was attenuated by heparin (Fig. 5G), as well as by pretreatment with chlorate (Fig. 5H) that depletes the major sulfate donor for sulfotransferase-dependent HS sulfation (31). These data provide the first biochemical and genetic evidence that stress-induced lipoprotein uptake in tumor cells is highly dependent on intact HSPG expression and HS sulfation.

Stress-induced cell signaling activation by lipoproteins depends on HSPGs

Although the primary role of lipoproteins is to transport lipids in the blood, they can also activate intracellular signaling pathways in vascular and stromal cells, in particular those involving the MAPKs (32), which have been widely implicated in tumor cell aggressiveness and as a therapeutic target of cancer (33). We initially addressed potential effects of lipoproteins at the level of intracellular kinase activation in glioblastoma cells. Both LDL and VLDL were shown to rapidly and transiently activate the ERK/MAPK pathway, as determined by increased ERK1/2 phosphorylation (Supplementary Fig. S6A). This notion was supported by increased activation of CREB and HSP27, which are known downstream targets of ERK1/2 (Supplemen-

tary Fig. S6A). Notably, HSPG-mediated endocytosis has been linked to downstream ERK/MAPK activation (34, 35). We found that increased ERK1/2 phosphorylation by LDL (Supplementary Fig. S6B) and VLDL (Supplementary Fig. S6C) was more pronounced in hypoxic as compared with normoxic glioblastoma cells. Interestingly, this effect was efficiently reversed by heparin (Fig. 6A). Similar results were obtained with wild-type CHO cells (Fig. 6B and C, left), while hypoxic induction of lipoprotein-mediated ERK1/2 phosphorylation was attenuated in HSPG-deficient cells (Fig. 6B and C, right). These data indicate a role for HSPGs as functionally relevant receptors in the context of hypoxia-induced, lipoprotein-mediated cell signaling activation.

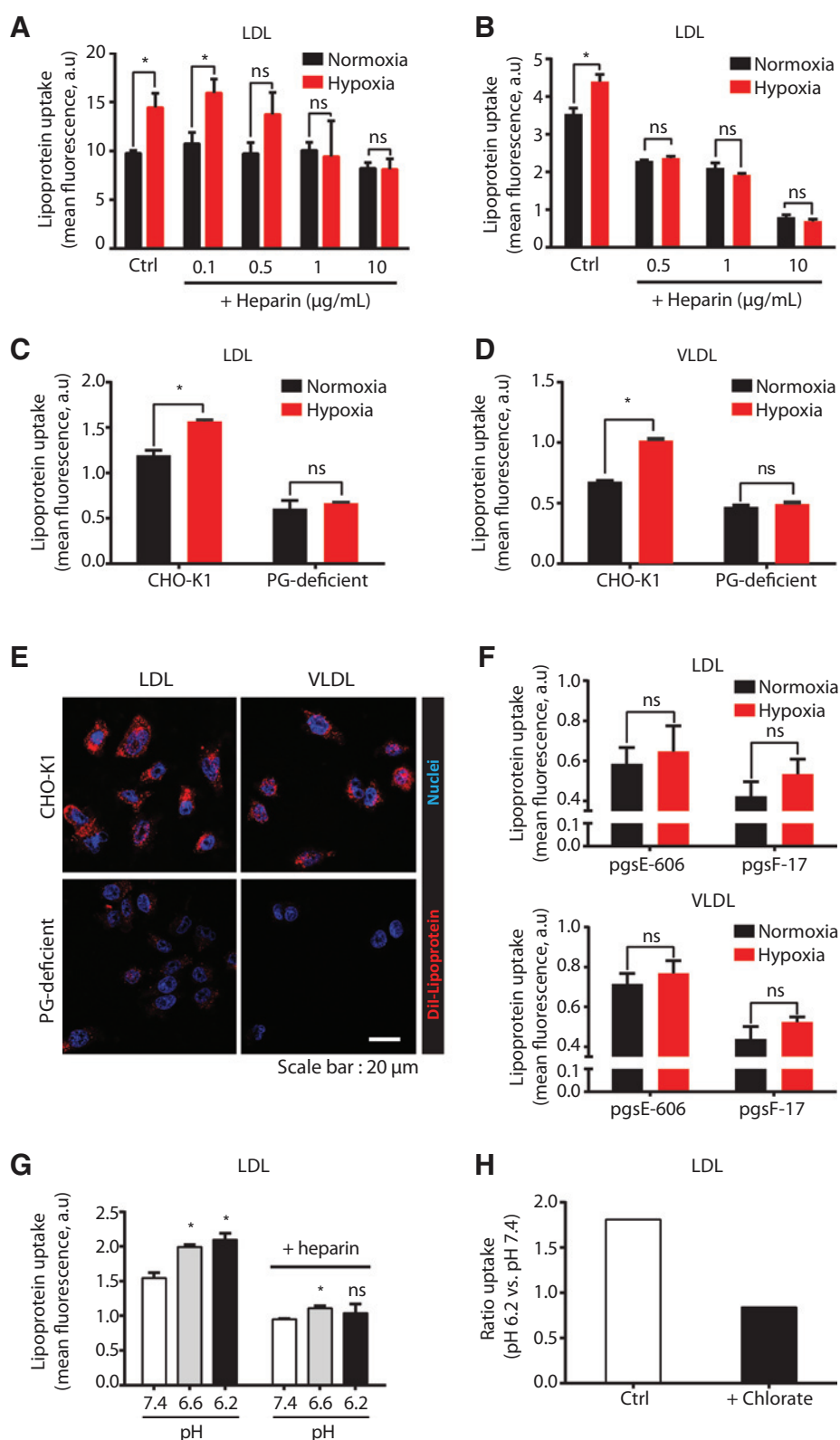
The lipid-loaded phenotype of stressed tumor cells depends on HSPGs

The above data indicated that HSPGs are required for stress-induced lipoprotein uptake. However, under stress conditions, a residual 20%–40% uptake activity remained in the presence of heparin and in HSPG-deficient mutant cells as compared with the respective controls (Fig. 5 and Supplementary Fig. S5E). Thus, we next investigated the functional relevance of HSPGs in lipoprotein-dependent formation of the LD-loaded phenotype. As expected, extracellular lipoproteins dramatically stimulated LD formation in hypoxic and acidic cells (Fig. 7A and B). Interestingly, heparin treatment was found to efficiently counteract lipoprotein-dependent LD formation in hypoxic as well as in acidic glioblastoma cells (Fig. 7A and B). Also, whereas hypoxic wild-type CHO cells displayed significant LD accumulation that was sensitive to heparin treatment, PG-deficient mutants showed very few LDs both in the absence and presence of heparin (Fig. 7C). These results clearly indicate that HSPGs are involved in extracellular lipid recruitment by tumor cells, and support the concept of an important functional role of HSPGs in stress-induced LD formation (Fig. 7D).

Discussion

Cancer is associated with dysregulated lipid metabolism both at the systemic and paracrine level and intracellular lipid accumulation may promote cancer cell aggressiveness (6, 36–38). Most studies involve the role of *de novo* lipogenesis from increased utilization of glucose carbons and autocrine processes, whereas the importance of extracellular lipids of the tumor microenvironment remains relatively ill-defined. However, solid tumors have access to circulating lipoproteins and increased systemic lipid levels have been associated with tumor development and progression (39). Here, we provide evidence for a novel role of HSPGs in the adaptive response of tumor cells to hypoxia and acidosis, which constitute major stress factors that characterize and drive tumor aggressiveness. We show that HSPGs are required for hypoxia and acidosis-induced internalization of lipoproteins, resulting in a lipid-storing phenotype that can promote spheroid formation and metastatic capacity. Furthermore, we show that lipoproteins trigger the ERK/MAPK pathway, which is a central signaling hub for the malignant cell phenotype (33), and that this effect is enhanced by hypoxia through an HSPG-dependent mechanism.

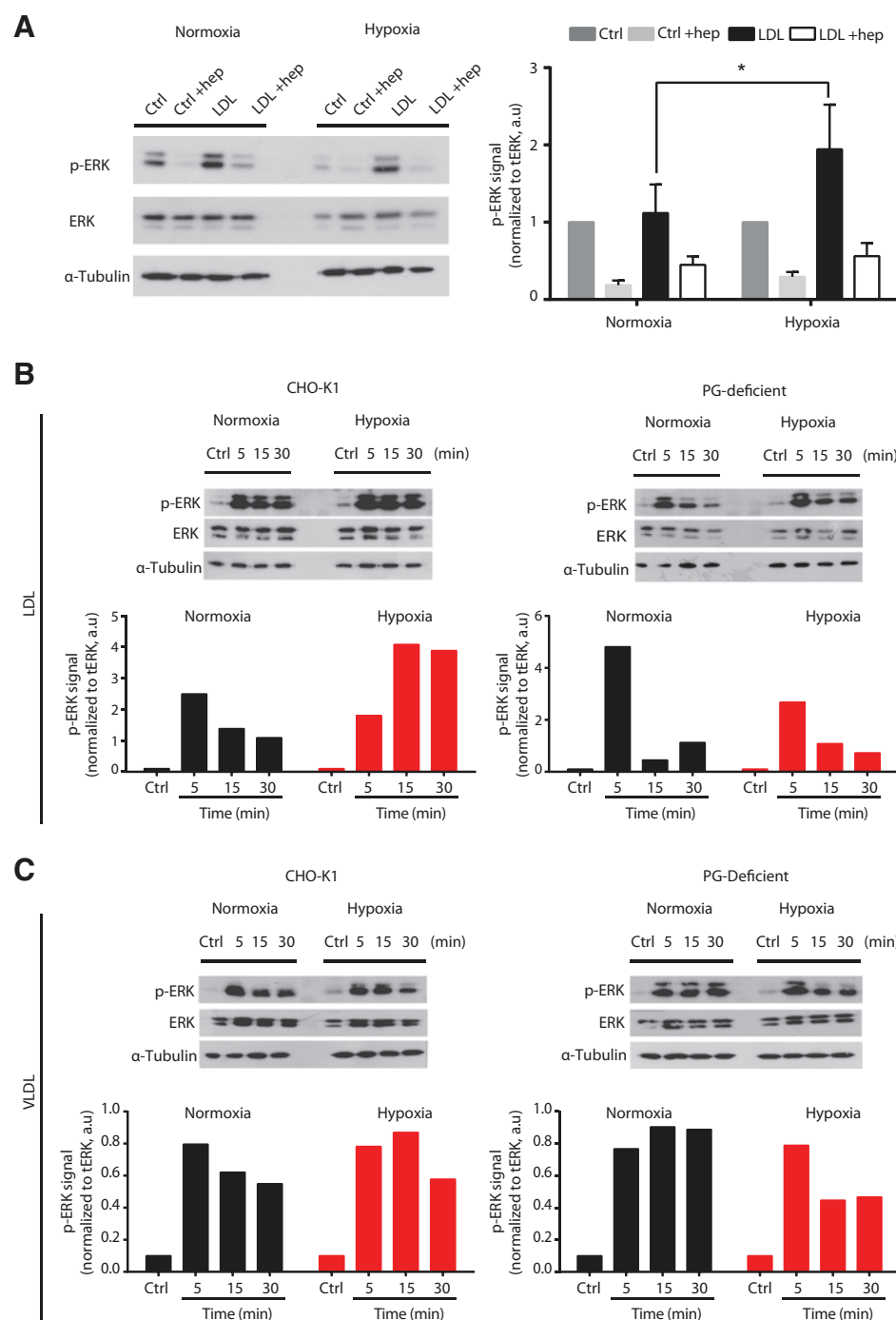
HSPGs are highly polyanionic glycosaminoglycans found at the surface of malignant and stromal tumor cells as well as in their surrounding matrix. The multifaceted role of HSPGs in,

**Figure 5.**

Hypoxia and acidosis-induced lipoprotein uptake is HSPG-dependent. **A** and **B**, U87-MG (**A**) and CHO (**B**) cells were incubated in normoxia or hypoxia for 2 hours and Dil-labeled LDL uptake (20 $\mu\text{g/mL}$ for 30 minutes) either in the absence or presence of heparin at the indicated concentrations was assessed by flow cytometry. **C** and **D**, uptake of Dil-labeled LDL (**C**) and VLDL (**D**) in hypoxic and normoxic wild-type (CHO-K1) and mutant (pgsA-745, PG-deficient) cells. **E**, decreased lipoprotein-positive intracellular vesicles in hypoxic, PG-deficient as compared with wild-type cells. Data shown are representative fields of triplicate experiments. **F**, uptake of Dil-labeled LDL (top) and VLDL (bottom) in normoxic and hypoxic pgsE-606 and pgsF-17 cells. **G**, U87-MG cells were incubated in neutral or acidic medium for 6 hours, and Dil-labeled LDL uptake either in the absence or presence of heparin (10 $\mu\text{g/mL}$) was determined. Data shown is representative of two independent experiments, each performed in triplicate. **H**, U87-MG cells were pretreated either with 25 mmol/L NaClO_3 to inhibit HS sulfation or the corresponding concentration of NaCl (Ctrl) for 24 hours, followed by incubated with Dil-labeled LDL in neutral or acidic medium, and analyzed for LDL uptake. Data are presented as fold of Ctrl (set to 1) from triplicates. **A–D** and **F**, data are presented as the mean \pm SD from three independent experiments, each performed in triplicate. *, $P < 0.05$. ns, nonsignificant.

for example, angiogenesis and metastasis has been extensively studied, and in some cases these functions are mediated through the facilitation of ligand endocytosis (23, 40). HSPG

internalization has been linked to activation of the MAPK pathway (41), which is notable considering our finding of HSPG-dependent ERK/MAPK induction by lipoproteins in

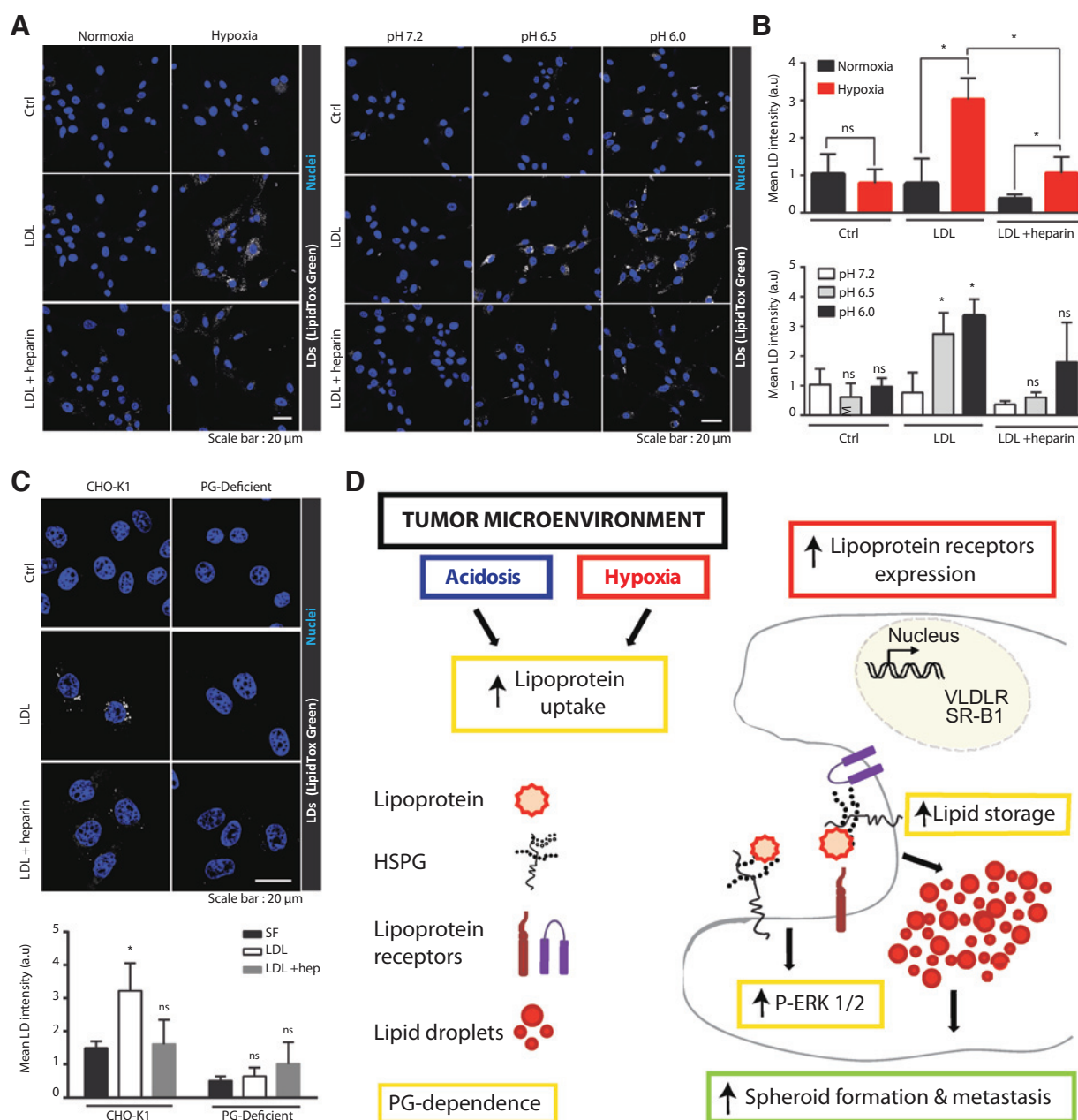
**Figure 6.**

Role of HSPGs in hypoxia-induced ERK/MAPK signaling activation by lipoproteins. **A**, U87-MG cells were incubated in normoxia or hypoxia for 2 hours, and then left untreated (Ctrl), or treated with LDL (50 μ g/mL), heparin (10 μ g/mL), or LDL and heparin for 15 minutes. Cell lysates were analyzed by immunoblotting for p-ERK1/2, and total ERK1/2 and α -tubulin were used as loading controls. Left, Western blot analysis from a representative experiment. Right, quantitative data of p-ERK1/2 normalized for total ERK1/2 and expressed as a ratio versus Ctrl (set to 1) in normoxia and hypoxia, respectively. Data are presented as the mean \pm SD from three independent experiments, each performed in triplicate. *, $P < 0.05$. **B** and **C**, wild-type CHO-K1 and HSPG-deficient pgsA-745 cells were grown in normoxia or hypoxia for 2 hours, and either left untreated (Ctrl), or treated with LDL (**B**) or VLDL (50 μ g/mL; **C**) for the indicated time points. Immunoblotting was performed as described above. Data shown are representative of three independent experiments.

hypoxic cells. HSPGs can act as autonomic internalizing receptors, be part of a multireceptor complex, or merely serve as an initial ligand attachment site. Accordingly, lipoprotein internalization could occur either independently of auxiliary receptors or act in concert with LRP1 and potentially other lipoprotein receptors, as suggested from numerous studies in nonmalignant cells (24, 25). Notably, we found that acidic stress is associated with increased lipoprotein uptake through both an induced mechanism, when cells were preincubated at acidic conditions, as well as through a direct mechanism when lipo-

protein uptake was performed in acidic medium. Indeed, the binding of LDL and VLDL to PGs may be increased at acidic pH (42), that is, induced uptake of lipoproteins in acidic medium could be due to increased interaction with cell surface HSPGs, as has been previously shown with LDL in macrophages (43).

Hypoxia was previously shown to regulate the expression of HS biosynthetic enzymes, resulting in increased responsiveness to FGF-2 (44), and altered expression of HSPGs has been described in several tumor types and may associate with their aggressiveness (40). Somewhat unexpectedly, we found that HSPG expression

**Figure 7.**

Dependence on HSPGs for stress-induced LD accumulation. **A**, U87-MG cells were grown in normoxia or hypoxia (left) or in neutral or acidic medium (right) in serum-free medium (Ctrl) or in the presence of LDL (50 μ g/mL) with or without heparin (100 μ g/mL). Shown are representative microscopy images of cells stained for LDs (white) and nuclei (blue). **B**, quantification of LD loading using CellProfiler, presented as the mean \pm SD from triplicate experiments; $n \geq 64$ cells for each condition. *, $P < 0.05$. ns, nonsignificant. **C**, top, representative confocal microscopy images from similar experiment as in **A** with hypoxic wild-type CHO-K1 and PG-deficient pgsA cells. Bottom, quantification of LD loading, presented as the mean \pm SD from triplicate experiments; $n \geq 53$ cells per condition. *, $P < 0.05$. **D**, proposed roles of HSPGs in tumor cell adaptation to tumor stress. Tumor cells respond to stress by (i) upregulated lipoprotein uptake, (ii) increased ERK/MAPK activation by lipoproteins, and (iii) increased intracellular lipid accumulation, which promotes spheroid formation and metastasis. The current study identifies a critical role of HSPGs in all of these responses.

and structural composition were unaffected at conditions associated with increased lipoprotein uptake and LD formation. Instead, major lipoprotein receptors were induced at the mRNA level in hypoxia, which was in accordance with an increased uptake of all major classes of lipoproteins, as well as with previous

studies showing hypoxic induction of VLDLR and LRP1 in other cell types (45–47). We found that at hypoxic conditions associated with increased lipoprotein uptake, VLDLR and SR-B1, but not LRP1, were also increased at the protein level, thus implicating SR-B1 and VLDLR as important in hypoxia-induced uptake of

VLDL, whereas SR-B1 should be involved in the increased uptake of LDL and HDL. Future studies that dissect out the respective roles of various lipoprotein receptors in stress-dependent induction of major lipoprotein classes and LD loading in malignant cells should be of interest. More importantly for the purpose of the current investigation, we found that the HSPG-dependent uptake route is highly relevant for the downstream biologic response to lipoproteins in stressed tumor cells, and interfering with HSPG levels was sufficient to abrogate stress-mediated upregulation of lipid uptake, cell signaling activation, and LD storage.

Enhanced lipoprotein uptake was shown in U87-MG cells expressing a mutated, constitutively active EGF receptor (EGFR-vIII), further resulting in PI3K-dependent induction of LDLR (48). We found LDLR not to be hypoxia-induced in glioblastoma tumors and U87-MG cells, which points at a complex interaction between oncogenic and nononcogenic events in glioblastoma tumor lipid metabolism. At present, we can only speculate about how oncogenic signaling and stress conditions collectively promote glioblastoma and other tumor types through increased lipoprotein uptake and LD accumulation. The most obvious is to provide energy to resist starvation and oxidative stress typically required for proliferation, survival, and migration. The tumorigenic effects of cholesterol may also be connected to increased lipid raft-dependent, protumorigenic signaling (49). Furthermore, lipoproteins carry substrates for the synthesis of prostaglandins that have been shown to promote tumor aggressiveness (50). Clearly, further mechanistic and functional studies will be needed to unravel the complex roles of lipid accumulation in the context of cell metabolism, membrane structure, and lipid signaling metabolites.

In summary, our data put HSPG-mediated macromolecular uptake into a new context that may be directly linked to a more protumorigenic cell phenotype. Clinical studies, in particular with lung cancer patients, suggest that heparin may have direct anti-tumor effects, and several ongoing trials will establish whether heparin should be added to the treatment arsenal against cancer (40). From our results, it may be proposed that the tumor-inhibiting effect of heparin is partly related to interference with cancer cell adaptation to stress conditions. This should further

motivate the identification of more specific therapeutic approaches targeted at the HSPG uptake machinery possibly as combined treatment with inhibitors of lipid synthesis.

Disclosure of Potential Conflicts of Interest

No potential conflicts of interest were disclosed.

Authors' Contributions

Conception and design: J. Menard, H.C. Christianson, M. Belting

Development of methodology: J. Menard, H.C. Christianson, K.J. Svensson, M. Belting

Acquisition of data (provided animals, acquired and managed patients, provided facilities, etc.): J. Menard, P. Kucharzewska, E. Bourseau-Guilmain, V.I. Chandran, L. Kjellén, C. Welinder, J. Bengzon

Analysis and interpretation of data (e.g., statistical analysis, biostatistics, computational analysis): J. Menard, H.C. Christianson, P. Kucharzewska, E. Bourseau-Guilmain, K.J. Svensson, V.I. Chandran, L. Kjellén, C. Welinder, M. Belting

Writing, review, and/or revision of the manuscript: J. Menard, H.C. Christianson, P. Kucharzewska, V.I. Chandran, J. Bengzon, M. Belting

Administrative, technical, or material support (i.e., reporting or organizing data, constructing databases): E. Lindqvist, M.C. Johansson

Study supervision: M. Belting

Acknowledgments

The authors thank Lina Gefors, Lund University for EM sample preparation and training, Dr. J.D. Esko for providing HS sulfation cell mutants, and Dr. T.H. van Kuppevelt for sharing AO4B09 anti-HS antibody.

Grant Support

This work was supported by The Swedish Cancer Fund, the Swedish Research Council, the Swedish Childhood Cancer Foundation, the Gunnar Nilsson, Anna Lisa and Sven Eric Lundgren, and Kamprad Foundations, the Skåne University Hospital donation funds, the Governmental funding of clinical research within the National Health Services, a donation by Viveca Jeppsson, and Region Skåne strategic position award.

The costs of publication of this article were defrayed in part by the payment of page charges. This article must therefore be hereby marked *advertisement* in accordance with 18 U.S.C. Section 1734 solely to indicate this fact.

Received October 18, 2015; revised April 5, 2016; accepted May 5, 2016; published OnlineFirst May 19, 2016.

References

- Pouyssegur J, Dayan F, Mazure NM. Hypoxia signaling in cancer and approaches to enforce tumour regression. *Nature* 2006;441:437–43.
- Bertout JA, Patel SA, Simon MC. The impact of O₂ availability on human cancer. *Nat Rev Cancer* 2008;8:967–75.
- Finger EC, Giaccia AJ. Hypoxia, inflammation, and the tumor microenvironment in metastatic disease. *Cancer Metastasis Rev* 2010;29:285–93.
- Brown JM, Wilson WR. Exploiting tumour hypoxia in cancer treatment. *Nat Rev Cancer* 2004;4:437–47.
- Neri D, Supuran CT. Interfering with pH regulation in tumours as a therapeutic strategy. *Nat Rev Drug Discov* 2011;10:767–77.
- Schulze A, Harris AL. How cancer metabolism is tuned for proliferation and vulnerable to disruption. *Nature* 2012;491:364–73.
- Koppenol WH, Bounds PL, Dang CV. Otto Warburg's contributions to current concepts of cancer metabolism. *Nat Rev Cancer* 2011;11:325–37.
- Semenza GL. Regulation of cancer cell metabolism by hypoxia-inducible factor 1. *Semin Cancer Biol* 2009;19:12–6.
- Pelletier J, Bellot G, Gounon P, Lacas-Gervais S, Pouyssegur J, Mazure NM. Glycogen synthesis is induced in hypoxia by the hypoxia-inducible factor and promotes cancer cell survival. *Front Oncol* 2012;2:18.
- Estrella V, Chen T, Lloyd M, Wojtkowiak J, Cornnell HH, Ibrahim-Hashim A, et al. Acidity generated by the tumor microenvironment drives local invasion. *Cancer Res* 2013;73:1524–35.
- Mosesson Y, Mills GB, Yarden Y. Derailed endocytosis: an emerging feature of cancer. *Nat Rev Cancer* 2008;8:835–50.
- Wang Y, Ohh M. Oxygen-mediated endocytosis in cancer. *J Cell Mol Med* 2010;14:496–503.
- Ausman JJ, Shapiro WR, Rall DP. Studies on the chemotherapy of experimental brain tumors: development of an experimental model. *Cancer Res* 1970;30:2394–400.
- Kurup S, Wijnhoven TJ, Jenniskens GJ, Kimata K, Habuchi H, Li JP, et al. Characterization of anti-heparan sulfate phage display antibodies AO4B08 and HS4E4. *J Biol Chem* 2007;282:21032–42.
- Nygren C, von Holst H, Mansson JE, Fredman P. Increased levels of cholesterol esters in glioma tissue and surrounding areas of human brain. *Br J Neurosurg* 1997;11:216–20.
- Clark MJ, Homer N, O'Connor BD, Chen Z, Eskin A, Lee H, et al. U87MG decoded: the genomic sequence of a cytogenetically aberrant human cancer cell line. *PLoS Genet* 2010;6:e1000832.
- Robenek H, Buers I, Hofnagel O, Robenek MJ, Troyer D, Severs NJ. Compartmentalization of proteins in lipid droplet biogenesis. *Biochim Biophys Acta* 2009;1791:408–18.
- Bostrom P, Magnusson B, Svensson PA, Wiklund O, Boren J, Carlsson LM, et al. Hypoxia converts human macrophages into triglyceride-loaded foam cells. *Arterioscler Thromb Vasc Biol* 2006;26:1871–6.

Menard et al.

19. Glinsky VV, Glinsky GV, Glinskii OV, Huxley VH, Turk JR, Mossine VV, et al. Intravascular metastatic cancer cell homotypic aggregation at the sites of primary attachment to the endothelium. *Cancer Res* 2003;63:3805–11.
20. Sodek KL, Ringuette MJ, Brown TJ. Compact spheroid formation by ovarian cancer cells is associated with contractile behavior and an invasive phenotype. *Int J Cancer* 2009;124:2060–70.
21. Hirschhaeuser F, Menne H, Dittfeld C, West J, Mueller-Klieser W, Kunz-Schughart LA. Multicellular tumor spheroids: an underestimated tool is catching up again. *J Biotechnol* 2010;148:3–15.
22. Kruth HS. Fluid-phase pinocytosis of LDL by macrophages: a novel target to reduce macrophage cholesterol accumulation in atherosclerotic lesions. *Curr Pharm Des* 2013;19:5865–72.
23. Christianson HC, Belting M. Heparan sulfate proteoglycan as a cell-surface endocytosis receptor. *Matrix Biol* 2014;35:51–5.
24. Mahley RW, Huang Y. Atherogenic remnant lipoproteins: role for proteoglycans in trapping, transferring, and internalizing. *J Clin Invest* 2007;117:94–8.
25. Foley EM, Esko JD. Hepatic heparan sulfate proteoglycans and endocytic clearance of triglyceride-rich lipoproteins. *Prog Mol Biol Transl Sci* 2010;93:213–33.
26. Wittrup A, Zhang SH, ten Dam GB, van Kuppevelt TH, Bengtson P, Johansson M, et al. ScFv antibody-induced translocation of cell-surface heparan sulfate proteoglycan to endocytic vesicles: evidence for heparan sulfate epitope specificity and role of both syndecan and glypican. *J Biol Chem* 2009;284:32959–67.
27. Schilling B, Rardin MJ, MacLean BX, Zawadzka AM, Frewen BE, Cusack MP, et al. Platform-independent and label-free quantitation of proteomic data using MS1 extracted ion chromatograms in skyline: application to protein acetylation and phosphorylation. *Mol Cell Proteomics* 2012;11:202–14.
28. Bai X, Crawford B, Esko JD. Selection of glycosaminoglycan-deficient mutants. *Methods Mol Biol* 2001;171:309–16.
29. Bame KJ, Zhang L, David G, Esko JD. Sulphated and undersulphated heparan sulphate proteoglycans in a Chinese hamster ovary cell mutant defective in N-sulphotransferase. *Biochem J* 1994;303(Pt 1):81–7.
30. Bai X, Esko JD. An animal cell mutant defective in heparan sulfate hexuronic acid 2-O-sulfation. *J Biol Chem* 1996;271:17711–7.
31. Belting M, Persson S, Fransson LA. Proteoglycan involvement in polyamine uptake. *Biochem J* 1999;338(Pt 2):317–23.
32. Dobrev I, Waeber G, Widmann C. Lipoproteins and mitogen-activated protein kinase signaling: a role in atherogenesis? *Curr Opin Lipidol* 2006;17:110–21.
33. Kamiyama M, Naguro I, Ichijo H. In vivo gene manipulation reveals the impact of stress-responsive MAPK pathways on tumor progression. *Cancer Sci* 2015;106:785–96.
34. Svensson KJ, Christianson HC, Wittrup A, Bourseau-Guilmain E, Lindqvist E, Svensson LM, et al. Exosome uptake depends on ERK1/2-heat shock protein 27 signaling and lipid Raft-mediated endocytosis negatively regulated by caveolin-1. *J Biol Chem* 2013;288:17713–24.
35. Christianson HC, Svensson KJ, van Kuppevelt TH, Li JP, Belting M. Cancer cell exosomes depend on cell-surface heparan sulfate proteoglycans for their internalization and functional activity. *Proc Natl Acad Sci U S A* 2013;110:17380–5.
36. Ackerman D, Simon MC. Hypoxia, lipids, and cancer: surviving the harsh tumor microenvironment. *Trends Cell Biol* 2014;24:472–8.
37. Cabodevilla AG, Sanchez-Caballero L, Nintou E, Boiadjeva VG, Picatoste F, Gubern A, et al. Cell survival during complete nutrient deprivation depends on lipid droplet-fueled beta-oxidation of fatty acids. *J Biol Chem* 2013;288:27777–88.
38. Bensaad K, Favaro E, Lewis CA, Peck B, Lord S, Collins JM, et al. Fatty acid uptake and lipid storage induced by HIF-1alpha contribute to cell growth and survival after hypoxia-reoxygenation. *Cell Rep* 2014;9:349–65.
39. Alikhani N, Ferguson RD, Novosyadlyy R, Gallagher EJ, Scheinman EJ, Yakar S, et al. Mammary tumor growth and pulmonary metastasis are enhanced in a hyperlipidemic mouse model. *Oncogene* 2013;32:961–7.
40. Iozzo RV, Sanderson RD. Proteoglycans in cancer biology, tumour micro-environment and angiogenesis. *J Cell Mol Med* 2011;15:1013–31.
41. Chen K, Williams KJ. Molecular mediators for raft-dependent endocytosis of syndecan-1, a highly conserved, multifunctional receptor. *J Biol Chem* 2013;288:13988–99.
42. Sneek M, Kovanen PT, Oorni K. Decrease in pH strongly enhances binding of native, proteolyzed, lipolyzed, and oxidized low density lipoprotein particles to human aortic proteoglycans. *J Biol Chem* 2005;280:37449–54.
43. Plihtari R, Kovanen PT, Oorni K. Acidity increases the uptake of native LDL by human monocyte-derived macrophages. *Atherosclerosis* 2011;217:401–6.
44. Li J, Shworak NW, Simons M. Increased responsiveness of hypoxic endothelial cells to FGF2 is mediated by HIF-1alpha-dependent regulation of enzymes involved in synthesis of heparan sulfate FGF2-binding sites. *J Cell Sci* 2002;115:1951–9.
45. Koong AC, Denko NC, Hudson KM, Schindler C, Swiersz L, Koch C, et al. Candidate genes for the hypoxic tumor phenotype. *Cancer Res* 2000;60:883–7.
46. Shen GM, Zhao YZ, Chen MT, Zhang FL, Liu XL, Wang Y, et al. Hypoxia-inducible factor-1 (HIF-1) promotes LDL and VLDL uptake through inducing VLDLR under hypoxia. *Biochem J* 2012;441:675–83.
47. Sundelin JP, Lidberg U, Nik AM, Carlsson P, Boren J. Hypoxia-induced regulation of the very low density lipoprotein receptor. *Biochem Biophys Res Commun* 2013;437:274–9.
48. Guo D, Reinitz F, Youssef M, Hong C, Nathanson D, Akhavan D, et al. An LXR agonist promotes glioblastoma cell death through inhibition of an EGFR/AKT/SREBP-1/LDLR-dependent pathway. *Cancer Discov* 2011;1:442–56.
49. Lingwood D, Simons K. Lipid rafts as a membrane-organizing principle. *Science* 2010;327:46–50.
50. Accioly MT, Pacheco P, Maya-Monteiro CM, Carrossini N, Robbs BK, Oliveira SS, et al. Lipid bodies are reservoirs of cyclooxygenase-2 and sites of prostaglandin- E-2 synthesis in colon cancer cells. *Cancer Res* 2008;68:1732–40.

Cancer Research

The Journal of Cancer Research (1916–1930) | The American Journal of Cancer (1931–1940)

Metastasis Stimulation by Hypoxia and Acidosis-Induced Extracellular Lipid Uptake Is Mediated by Proteoglycan-Dependent Endocytosis

Julien A. Menard, Helena C. Christianson, Paulina Kucharzewska, et al.

Cancer Res 2016;76:4828-4840. Published OnlineFirst May 19, 2016.

Updated version Access the most recent version of this article at:
doi:[10.1158/0008-5472.CAN-15-2831](https://doi.org/10.1158/0008-5472.CAN-15-2831)

Supplementary Material Access the most recent supplemental material at:
<http://cancerres.aacrjournals.org/content/suppl/2016/05/19/0008-5472.CAN-15-2831.DC1>

Cited articles This article cites 50 articles, 21 of which you can access for free at:
<http://cancerres.aacrjournals.org/content/76/16/4828.full#ref-list-1>

Citing articles This article has been cited by 1 HighWire-hosted articles. Access the articles at:
<http://cancerres.aacrjournals.org/content/76/16/4828.full#related-urls>

E-mail alerts [Sign up to receive free email-alerts](#) related to this article or journal.

Reprints and Subscriptions To order reprints of this article or to subscribe to the journal, contact the AACR Publications Department at pubs@aacr.org.

Permissions To request permission to re-use all or part of this article, use this link
<http://cancerres.aacrjournals.org/content/76/16/4828>.
Click on "Request Permissions" which will take you to the Copyright Clearance Center's (CCC) Rightslink site.